Matrix Metalloproteinase-1-mediated Up-regulation of Vascular Endothelial Growth Factor-2 in Endothelial Cells[*]

Rafi Mazor[‡1,2], Tom Alsaigh[‡1,3], Helena Shaked[§], Angelina E. Altshuler[‡], Elizabeth S. Pocock[¶], Erik B. Kistler[‡||**], Michael Karin[§], and Geert W. Schmid-Schönbein[‡]

From the [‡]Department of Bioengineering, The Institute of Engineering in Medicine, and the [¶]Department of Surgery and [||]Anesthesiology Service, Veterans Affairs Medical Center, San Diego, California, [**]Department of Anesthesiology and Critical Care, University of California, San Diego, La Jolla, California, and the [§]Laboratory of Gene Regulation and Signal Transduction, School of Medicine, University of California San Diego, MC 0723, La Jolla, California 92093-0723

Background: Matrix metalloproteinases (MMP) and VEGFR2 often coexist in many settings, but their interactions are unknown.
Results: MMP-1 stimulates VEGFR2 up-regulation in endothelial cells.
Conclusion: MMP-1-stimulated cells have elevated intracellular signaling and proliferate at a faster rate than unstimulated cells.
Significance: A novel mechanism is uncovered whereby MMP-1 is able to sensitize endothelial cell functions.

Matrix metalloproteinase-1 (MMP-1) is a collagenase that is highly active in extracellular matrix and vascular remodeling, angiogenesis, and tumor progression. Vascular endothelial growth factor receptor-2 (VEGFR2), the main receptor for VEGF-A, is expressed on endothelial cells and promotes cell survival, proliferation, and other functions. Although MMP-1 and VEGFR2 co-exist in many normal and pathophysiological conditions, the effect of MMP-1 on cellular VEGFR2 that can promote the above processes is unknown. In this study we test the hypothesis that stimulation of endothelial cells with MMP-1 increases their levels of VEGFR2. The increased VEGFR2 is then available to bind VEGF-A, resulting in increased response. Indeed we found that endothelial cells incubated with active MMP-1 had higher mRNA and protein levels of VEGFR2. Furthermore, VEGF-A-dependent phosphorylation of intracellular signaling molecules and endothelial proliferation were elevated after MMP-1 treatment. MMP-1 caused activation of the nuclear factor-κB (NF-κB) pathway (p65/RelA) in endothelial cells, and this response was dependent upon activation of protease activated receptor-1 (PAR-1). Chromatin immunoprecipitation was used to confirm NF-κB-mediated active transcription of the VEGFR2 (*KDR*) gene. Elevation in VEGFR2 after MMP-1 stimulation was inhibited by PAR-1 knockdown and NF-κB specific inhibition. We conclude that MMP-1 promotes VEGFR2 expression and proliferation of endothelial cells through stimulation of PAR-1 and activation of NF-κB. These results suggest a mechanism by which MMP-1 may prime or sensitize endothelial cell functions.

Matrix metalloproteinases (MMPs)[4] are a family of zinc-dependent proteases that were originally characterized by their ability to degrade components of the extracellular matrix. These proteases can also act together with the endothelium to facilitate responses such as vascular remodeling, wound healing, cell invasion, permeability, proliferation, and survival (1–8). A major receptor on endothelial cells that governs these responses is VEGFR2, a receptor tyrosine kinase that readily undergoes tyrosine phosphorylation and receptor dimerization upon ligand stimulation (9–11). VEGF-A-mediated stimulation of VEGFR2 leads to activation of extracellular signal-related kinase 1/2 (ERK1/2), JNK, MAPK (p38), and others (11, 12). Collectively these signaling molecules modulate a variety of endothelial functions, including endothelial survival, permeability, and proliferation (7, 13, 14).

Among the different MMPs, MMP-1 (an interstitial collagenase capable of degrading collagen types I, II, and III) has been positively correlated with certain cancers (15–20), is a biomarker for venous disease (21–23), and has a role in modulating endothelial permeability (4–6). Among the many substrates for MMP-1, protease-activated receptor-1 (PAR-1) has been shown to play an important role in endothelial cell functions and blood vessel development (24–27). Additionally, it was shown that activation of PAR-1 by the serine protease thrombin enhances endothelial levels of VEGFR228, thus suggesting a key role for PAR-1 in endothelial cell functions. Given the frequent interactions MMPs have with the endothelium, it is possible that a mechanism exists by which MMPs may serve to sensitize endothelial cells for VEGFR2-mediated functions.

[1] Both authors contributed equally to this work.
[2] To whom correspondence may be addressed. Tel.: 858-534-3852; Fax: 858-534-5722; E-mail: rmazor@eng.ucsd.edu.
[3] To whom correspondence may be addressed. Tel.: 858-534-3852; Fax: 858-534-5722; E-mail: tom.alsaigh@gmail.com.

[4] The abbreviations used are: MMP, matrix metalloproteinase; HUVEC, human umbilical venous endothelial cell; BAEC, bovine aortic endothelial cell; PAR-1, protease activated receptor-1.

Therefore, in the present study we specifically tested whether endothelial cell stimulation with MMP-1 would result in up-regulation of VEGFR2 expression and therefore augment VEGF-A-mediated signaling, thereby enhancing the proliferative response. We were able to show that cells treated with MMP-1 have increased levels of VEGFR2. By the use of specific inhibition protocols we also found that the mechanism by which VEGFR2 is up-regulated is mediated by PAR-1 and activation of the NF-κB pathway. These results therefore provide insights regarding the ability of MMP-1 to enhance endothelial functions/activities in conditions associated with increased levels of MMP-1.

EXPERIMENTAL PROCEDURES

Cell Culture, Treatments, and Reagents

Human umbilical venous endothelial cells (HUVECs) were purchased from Cell Applications, Inc., and bovine aortic endothelial cells (BAECs) were a generous gift from Dr. Shu Chien (University of California San Diego). All cells were used between passages 2 and 4. HUVECs and BAECs were cultured in complete growth media (Cell Applications Inc.) at 37 °C and 5% CO_2. At subconfluence, cells were starved overnight in serum-free maintenance media (Cell Applications Inc.) to reach a baseline level of gene expression. To evaluate changes in VEGFR2 expression over time, cells were incubated with 25 ng/ml of MMP-1 (EMD Biosciences) activated with 4-aminophenylmercuric acetate (10:1, respectively, at 37 °C for 2 h) at appropriate time points. MMP-1 activity levels were measured before each experiment and kept constant for all experiments. MMP-8 and MMP-9 were purchased by EMD Biosciences and activated as described. NF-κB, IκB, P-IκB, Histone H3, ERK, P-ERK, JNK, P-JNK (Thr^{183}/Tyr^{185}), MAPK, P-MAPK (Thr^{180}/Tyr^{182}), and P-VEGFR2 (Tyr^{1175}) antibodies were ordered from Cell Signaling Technology, Inc., and were used 1:1000 in 0.5% TBS-T in 5% nonfat milk blocking reagent for Western blotting. VEGFR2 and β-actin primary antibodies were purchased from Santa Cruz Biotechnology and used 1:1000 as described above for Western blotting. FITC-conjugated chicken anti-human VEGFR2 antibody used for immunofluorescence was purchased from Genetex and was used 1:100 in 5% normal goat serum in PBS. PAR-1 primary antibody was purchased from Beckman Coulter and used for Western blotting as described. RNAi transfections were performed as indicated by the manufacturer with siRNA transfection reagent, siRNA transfection medium, control fluorescein siRNA, and human thrombin receptor siRNA (Santa Cruz Biotechnology, Inc.). VEGF-A was purchased from PeproTech and used at 5 ng/ml. To inhibit the NF-κB pathway, CAY 10512 (0.15 μM; Cayman) was used.

Cell Lysis and Nuclear Separations

For VEGFR2 and signaling proteins analysis, cells were lysed on ice with RIPA buffer supplemented with protease and phosphatase inhibitors (mixtures; Sigma and Pierce). For NF-κB analysis, endothelial cells were stimulated with MMP-1 for predetermined time points, then harvested and lysed with 20 mM Tris-HCl (pH 7.5), 0.5% Triton X-100, 0.5 mM Na$_3$VO$_4$, 10% glycerol, 1 mM EDTA, 1 mM EGTA, and 50 mM NaF to obtain cytosolic fractions. After centrifugation, pellets were then lysed with the described lysis buffer supplemented with 2.5% Triton

X-100 detergent for lysis of nuclear fractions. These fractions were used for Western blotting to determine nuclear levels of p65. For experiments where NF-κB was inhibited, cells were treated with 0.15 μM NF-κB inhibitor (CAY10512) overnight in serum-free media. Cells were then harvested and nuclear and cytoplasmic fractions were separated as described above.

Immunofluorescence

Cells were grown to subconfluence in 96-well tissue culture plates (BD Falcon).

VEGFR2—To test for elevated protein expression, HUVECs were treated with MMP-1 in serum-free media for 0, 4, 8, 12, and 24 h and BAECs were treated for 0, 1, 3, 6, and 24 h.

NF-κB—Both cell types were serum starved for 2 h and subsequently treated with MMP-1 for 0, 5, 15, 30, or 60 min, or TNF-α for 30 min. After treatment cells were fixed with 2% paraformaldehyde (for membrane VEGFR2 staining) or with ice-cold methanol (whole cell staining) for 20 min at room temperature. Cells were incubated with primary antibody against VEGFR2, NF-κB (p65 subunit), and/or β-tubulin in 5% normal goat serum in PBS for 1 h. Cells were washed with 1$\times$ PBS and then incubated with either FITC-conjugated secondary antibody, or Texas Red Avidin-D. Nuclei were stained with DAPI.

High Throughput Imaging and Analysis

Imaging was carried out using the Opera QEHS system (PerkinElmer Life Sciences) at the Sanford Burnham Medical Research Institute CPCCG with objective: $\times$20, 0.45 NA (Numerical Aperture). Channel 1 (nucleus) nuclei were stained with DAPI. The DAPI channel was imaged using the nonconfocal light path. The Opera's xenon arc lamp set to 365 nm was used for excitation and an emission filter of 450/50 nm was used in front of the camera. The exposure time for channel 1 was ~40 ms. For channel 2 (FITC), the cytoplasm/membrane was excited using the 488-nm laser line. The images were acquired using the confocal system of the Opera QEHS system. The exposure time was ~2000 ms. Nine fields were acquired for each well. The image analysis was done using Acapella 2.5. The analysis algorithm was developed at the Conrad Prebys Centre for Chemical Genomics (CPCCG). The algorithm uses inbuilt Nuclei, Membrane, and Cytoplasm detection.

Bromodeoxyuridine (BrdU) Proliferation Assay

To examine the ability of MMP-1 to prime endothelial cells for proliferation, we measured BrdU incorporation after MMP-1 treatment using a commercial kit (Roche Applied Science). Cells were grown in 96-well plates (BD Biosciences) and transferred to starvation media with/without MMP-1 for 24 h. Starvation media was then removed and complete media was supplemented with 10 ng/ml of VEGF-A and BrdU was added for 5 h. Cells were fixed and labeled for BrdU according to the manufacturer's protocol.

PAR-1 siRNA Transfections

Briefly, subconfluent HUVECs were transfected with 40 pmol of human PAR-1 siRNA or control fluorescein conjugate siRNA using siRNA transfection reagent (SCB, Inc.). Cells were incubated only with transfection reagents for 5 h. Complete

TABLE 1
qPCR and ChIP primers used

	Forward primer (5′ - 3′)	Reverse primer (5′ - 3′)
RT-PCR primers (BAEC)		
Flk1	TGG CAT CAC GGA AGT GTA TCC	CGG GCC AAG CCAAAG TC
β-Actin	GCG TGG CTA CAG CTT CAC	TTG ATG TCA CGG ACGATT TC
RT-PCR primers (HUVEC)		
KDR	CTGACGATTATGGAAGTGAGTGAAA	TGGCTCTGCTTCTCCTTTGAA
β-Actin	CTGGAACGGTGAAGGTGACA	AAGGGACTTCCTGTAACAATGCA
ChIP primers (HUVEC)		
KDRp1	CAAAAGGGCAAGTTCACCAT	GGCAGAGAATGAAGGTCTGG
KDRp2	CCACTCGGCTACCAAAATCA	TGGCATAGTCTCAGCTTCCT
KDRp6	ATTTCCCCACACAACTGGAC	GGCAAGCGATTAAATCTTGG
RANTES	CTTATGATACCGGCCAATGC	GTGCGAGGTCCACGTGCTGTC
β-Actin	ACTGCTGGGTAGGTTTGTAGCCTTCATCA	TAGCTAAATGTGCTGGGTGGGTCA

media was subsequently added to the mixture with the cells exposed to siRNA complexes overnight. The next day the transfection media was removed and replaced with complete media. Cells were assayed for PAR-1 expression 48 h post-transfection.

Western Blotting and Cellular Signaling

For cellular signaling analysis cells were treated with MMP-1 for 24 h followed with 5 ng/ml of recombinant VEGF-A (PeproTech) for 5 and 15 min in serum-free maintenance media, washed with PBS, and lysed for analysis. For each experiment, 40 μg of total protein was separated by SDS-PAGE and transferred onto nitrocellulose membranes. Membranes were blocked with 5% nonfat milk in Tris-buffered saline (pH 7.4) with 0.5% Tween 20 (TBS-T). Blots were then incubated overnight at 4 °C in TBS-T, 5% milk containing primary antibodies against the studied proteins. Blots were then washed and incubated with HRP-conjugated secondary antibodies. Signal on x-rays films was detected using the chemiluminescence reagents of the EZ-ECL kit (Pierce). Band density was analyzed using the NIH Image J software.

Quantitative Real Time-PCR

For mRNA analysis, cells were lysed and genetic material was purified according to the manufacturer's protocols (Qiagen). cDNA templates were generated from 3 μg of RNA using SuperScript III Reverse Transcriptase (Invitrogen). Quantitative RT-PCR were performed using the ABI Prism 7900HT Thermal Cycler, using primers for VEGFR2 (*Flk-1* in BAEC or *KDR* in HUVEC) and β-actin as a normalization control (Table 1). Data analysis was performed using Applied Biosystems Sequence Detection System (SDS) software.

Chromatin Immunoprecipitation

Briefly, cells (20 million per ChIP reaction) were treated with MMP-1 for 30 min or left untreated; then fixed with 1% formaldehyde for 10 min at room temperature, lysed and sonicated producing 300–400-bp DNA fragments. A sample of input DNA was saved and p65 was precipitated overnight with anti-rabbit DynaBeads (Invitrogen) pre-coupled with 10 mg of anti-p65 antibody (Santa Cruz sc-372). The beads were extensively washed and DNA was eluted, and the cross-links were reversed at 65 °C for 6 hr, after which both immunoprecipitated and input DNA fractions were treated with Proteinase K. DNA was recovered using Qiagen PCR product purification kit and subjected to gene-specific quantitative real time-PCR with the indicated primers (Table 1). To estimate the assay background, normal rabbit IgG (Santa Cruz sc-2027) was used instead of the p65 antibody; the levels of *KDR* regions precipitated with p65 antibody in the untreated cells were similar to those precipitated with the normal IgG (data not shown).

Statistical Analysis

All statistical results were presented as mean ± S.E. An unpaired two-tailed Student's *t* test was used for comparison between two groups. Analysis of variance was used to test for differences in outcomes of interest among groups. Results were determined to be significant at (*) $p < 0.05$. Tukey's post-hoc multiple comparison test was used to determine the significance between individual groups. All analyses were performed using SPSS version 18, Chicago, IL.

RESULTS

MMP-1 Stimulation Augments VEGFR2 Levels in Endothelial Cells

Protein—Membrane-associated VEGFR2 is increased in a temporal fashion following stimulation with MMP-1 (245 ± 12.2 mean fluorescent intensity at $t = 0$ *versus* 346 ± 28.8 mean fluorescent intensity at $t = 24$ h, *, $p < 0.05$; Fig. 1, *A* and *B*). Whole cell VEGFR2 levels were also increased after treatment with MMP-1 (1.5 ± 0.28 *versus* 0.68 ± 0.07 Relative Density Units of MMP-1 treated *versus* untreated cells; $p < 0.05$; Fig. 1, *C* and *D*).

mRNA—VEGFR2/*KDR* gene transcript levels were elevated following treatment with MMP-1 for 30 min and 8 h (3 ± 0.2 at 30 min and 4.4 ± 0.6-fold amplification at 8 h *versus* 1 ± 0.3 at $t = 0$; *, $p < 0.05$; Fig. 1*E*). In BAECs, as in HUVECs, VEGFR2 protein and *VEGFR2/Flk-1* mRNA levels were significantly higher after MMP-1 treatment compared with untreated control cells (Fig. 1, *F–H*).

MMP-1 Augments VEGF-A-dependent Signaling

Control and MMP-1-treated cells were stimulated with VEGF-A for 5 and 15 min to examine the ability of newly expressed VEGFR2 to enhance VEGF-A-mediated signaling levels (Fig. 2). At both 5 and 15 min following stimulation with VEGF, phosphorylation levels of the target proteins VEGFR2, ERK (0.95 ± 0.01 *versus* 0.7 ± 0.02, $p < 0.05$; Fig. 2*C*), and JNK and MAPK were significantly higher in MMP-1-treated cells *versus* controls (Fig. 2, *A–C*). Phosphorylated VEGFR2 levels relative to β-actin loading controls were significantly elevated
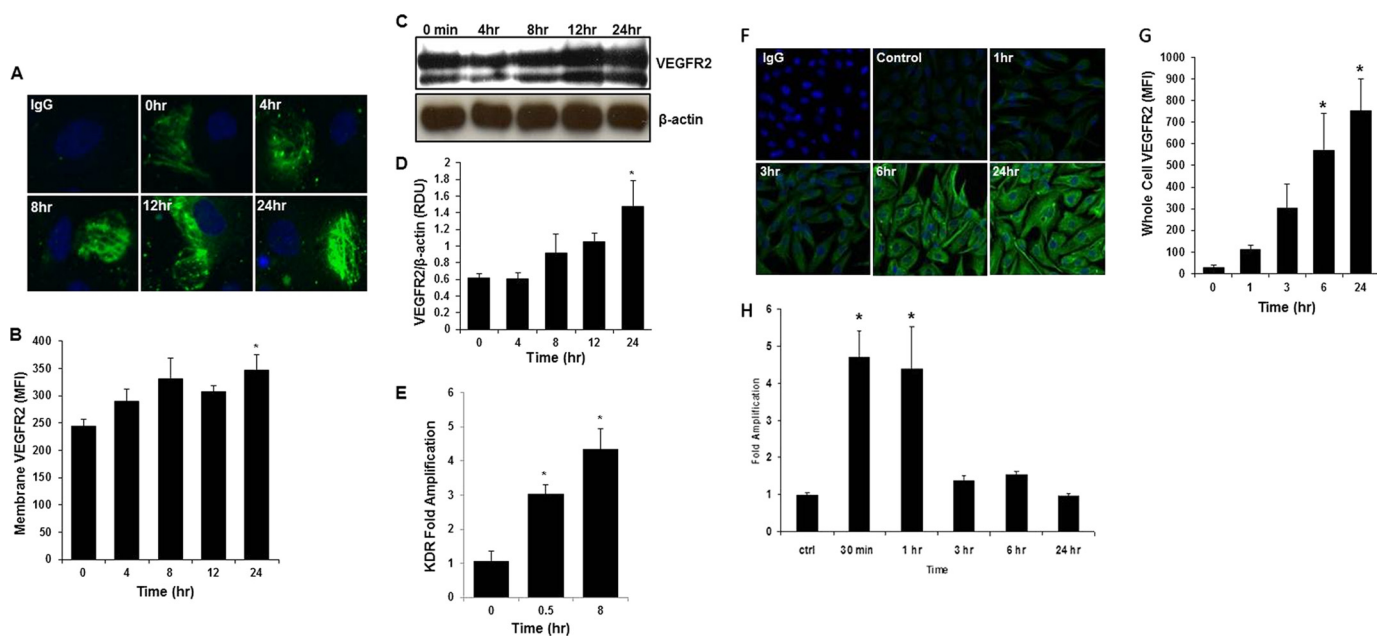
FIGURE 1. **MMP-1 increases the expression of VEGFR2 on endothelial cells.** *A,* confocal images of *membrane* labeling of VEGFR2 (*green; blue* = DAPI nuclear stain) in PAF fixed HUVECs. Time points indicate the length of incubation with MMP-1. *B,* high throughput confocal laser scanning analysis of VEGFR2 membrane mean fluorescent intensity (*MFI*) before and after MMP-1 treatment (~500 cells/well were counted in the analysis, $n = 4$, *, $p < 0.05$). *C,* representative Western blot, and *D,* quantification depicting increasing levels of whole cell VEGFR2 in HUVECs after MMP-1 treatment for the indicated time points ($n = 4$). *E,* VEGFR2 mRNA levels in HUVECs after the indicated time of treatment with MMP-1 ($n = 4$). *F,* confocal images of methanol-fixed BAECs immunolabeled for *whole cell* VEGFR2 at different incubation times with MMP-1. *G,* high throughput confocal laser scanning analysis of whole cell VEGFR2 levels (~500 cells/well were counted in the analysis, $n = 4$, *, $p < 0.05$). *H,* real-time PCR analysis of VEGFR2 mRNA levels in BAECs before and after MMP-1 stimulation. Results are presented as -fold amplification normalized to endogenous levels of β-actin ($n = 3$, *, $p < 0.05$).
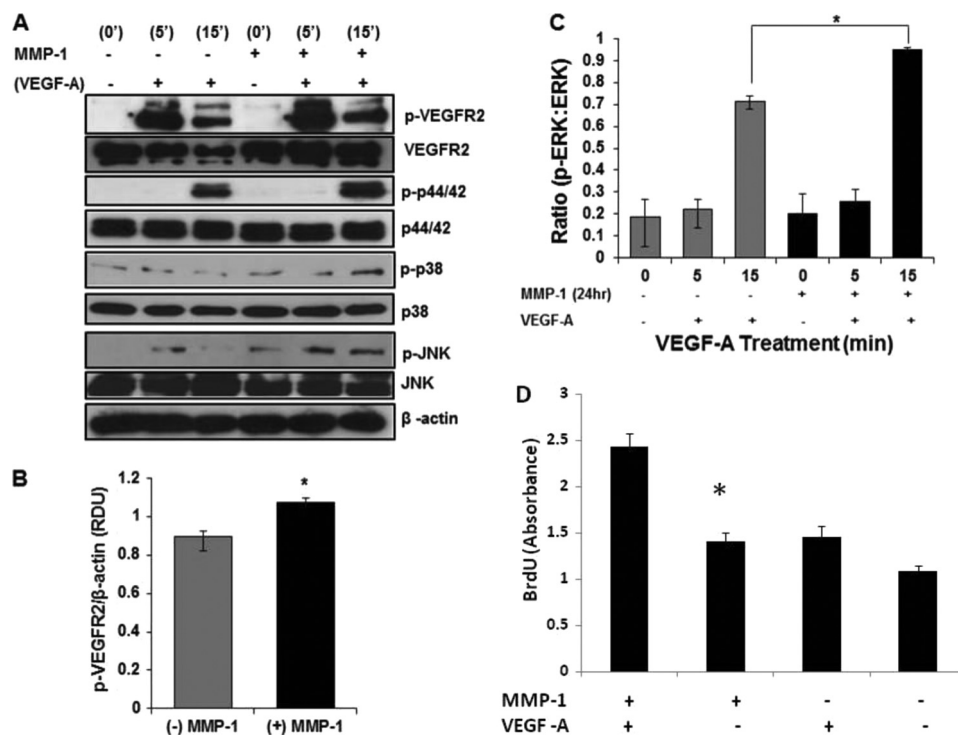

FIGURE 2. **MMP-1 stimulation augments VEGF-A-mediated signaling and endothelial proliferation.** *A,* representative Western blot of phosphorylated signaling proteins (VEGFR2, ERK, JNK, and MAPK) from HUVECs treated overnight with or without MMP-1 followed by treatment with 10 ng/ml of VEGF-A for the indicated time points. *B,* densitometry measurements of *p*-VEGFR2 (after 5 min of VEGF-A stimulation) with (*black*) and without (*gray*) MMP-1 treatment for 24 h. Standardization is against levels of β-actin ($n = 6$, *, $p < 0.05$). *C,* band density ratio between the phosphorylated protein divided by total protein for ERK ($n = 3$, *, $p < 0.05$). *D,* BrdU values for cells treated with ($n = 16$ wells; 500cells/well) and without ($n = 9$ wells; 500 cells/well) MMP-1 for 24 h before BrdU incorporation and fixation (*, $p < 0.05$).
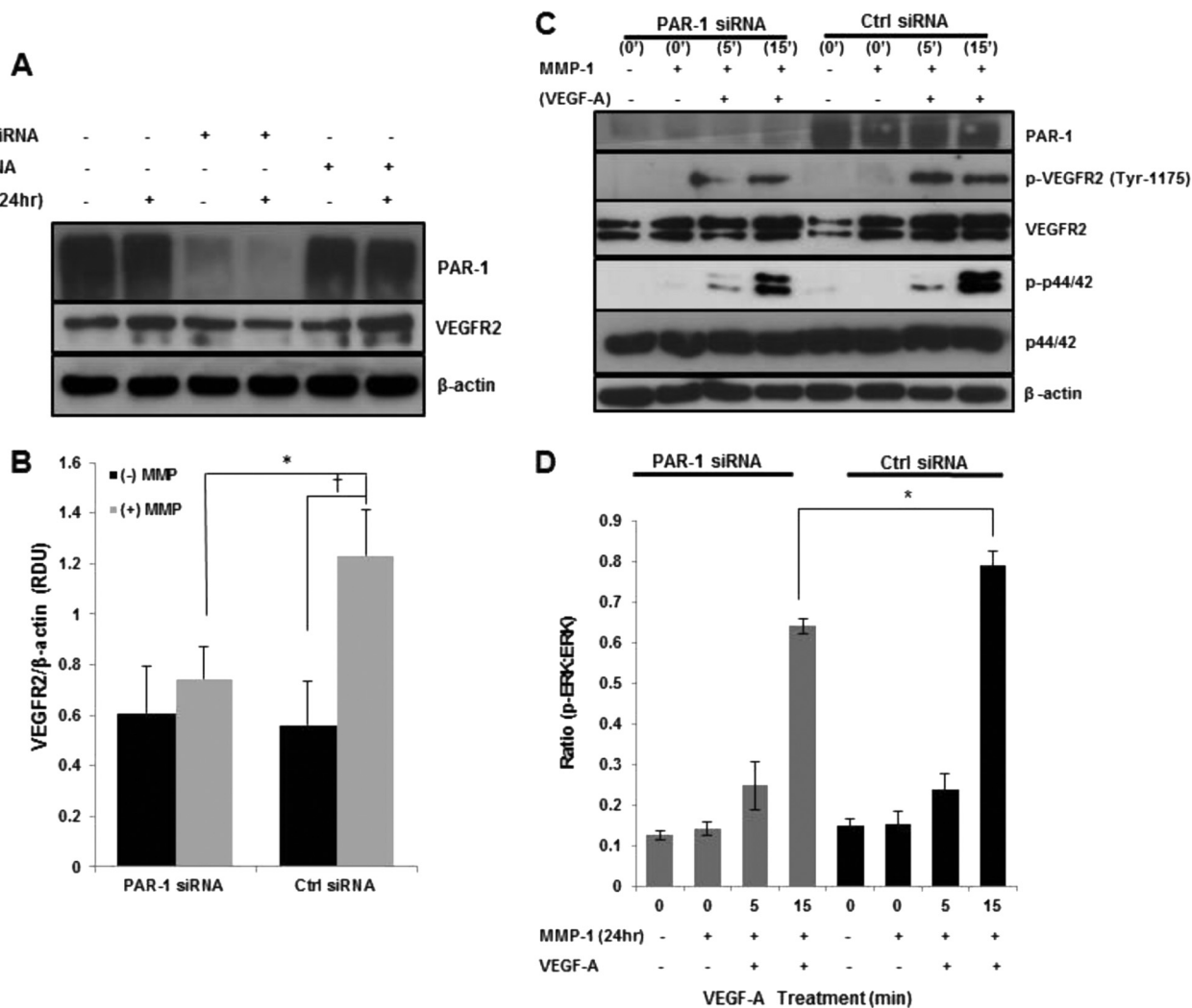
FIGURE 3. **PAR-1 silencing attenuates MMP-1-mediated VEGFR2 up-regulation.** *A*, representative Western blot displaying VEGFR2 levels in PAR-1 and control siRNA-transfected cells treated with or without MMP-1 ($n = 3$). *B*, quantified VEGFR2 levels after MMP-1 stimulation of PAR-1 knockdown and control cells ($n = 3$; *, $p < 0.05$; †, $p < 0.05$). *C*, representative Western blot displaying VEGF-A-mediated *p*-VEGFR2 and *p*-ERK signaling levels following corresponding transfections and 24 h treatment with MMP-1 ($n = 3$). *D, bar graph* depicts the band density ratio between the phosphorylated protein divided by total protein for ERK ($n = 3$, *, $p < 0.05$).

following a 24-h MMP-1 treatment and 5-min incubation with VEGF-A (Fig. 2, *A* and *B*; $n = 6$; *, $p < 0.05$).

Endothelial Cell Proliferation Is Enhanced following MMP-1 Treatment

To measure one possible physiologic outcome that an increase in VEGFR2 due to MMP-1 stimulation might have, we measured cell proliferation via BrdU incorporation after stimulation with MMP-1. Our results (Fig. 2*D*) show that cells treated with MMP-1 and then stimulated with VEGF-A proliferate at a significantly faster rate compared with untreated cells exposed to VEGF-A.

PAR-1 Knockdown Attenuates the Increase of VEGFR2 Protein and Signaling Levels

As a known substrate for MMP-1 (25), we next examined whether or not PAR-1 was responsible for the MMP-1-mediated increase in VEGFR2 levels. PAR-1 knockdown blunted the otherwise increased VEGFR2 levels upon 24 h of MMP-1 treatment seen in cells transfected with control siRNA (0.75 ± 0.17

versus 1.24 ± 0.18 Relative Density Units, respectively, $p < 0.05$; Fig. 3, *A* and *B*). Moreover, cells transfected with control siRNA had increased levels of VEGFR2 following MMP-1 stimulation for 24 h compared with untreated cells (1.24 ± 0.18 *versus* 0.56 ± 0.13 RDU, respectively, $p < 0.05$; Fig. 3, *A* and *B*). Upon stimulation with VEGF-A, phosphorylated VEGFR2 was decreased at 5 and 15 min in PAR-1 knockdowns (Fig. 3*C*) compared with control cells expressing PAR-1. Due to its prominent role in endothelial proliferation (7), we chose to focus on the effect PAR-1 knockdown has on ERK signaling following MMP-1 treatment. At 15 min of VEGF-A treatment, levels of *p*-ERK were significantly lower in MMP-1-treated PAR-1 knockdown cells compared with MMP-1-treated control siRNA-transfected cells (0.64 ± 0.02 *versus* 0.79 ± 0.04 RDU, respectively, $p < 0.05$; Fig. 3, *C* and *D*).

NF-κB Is Activated and Responsible for Modulation of VEGFR2 Levels following MMP-1 Stimulation

Upon stimulation with MMP-1 for 30 min, immunostaining depicts nuclear translocation of the p65/RelA subunit into the
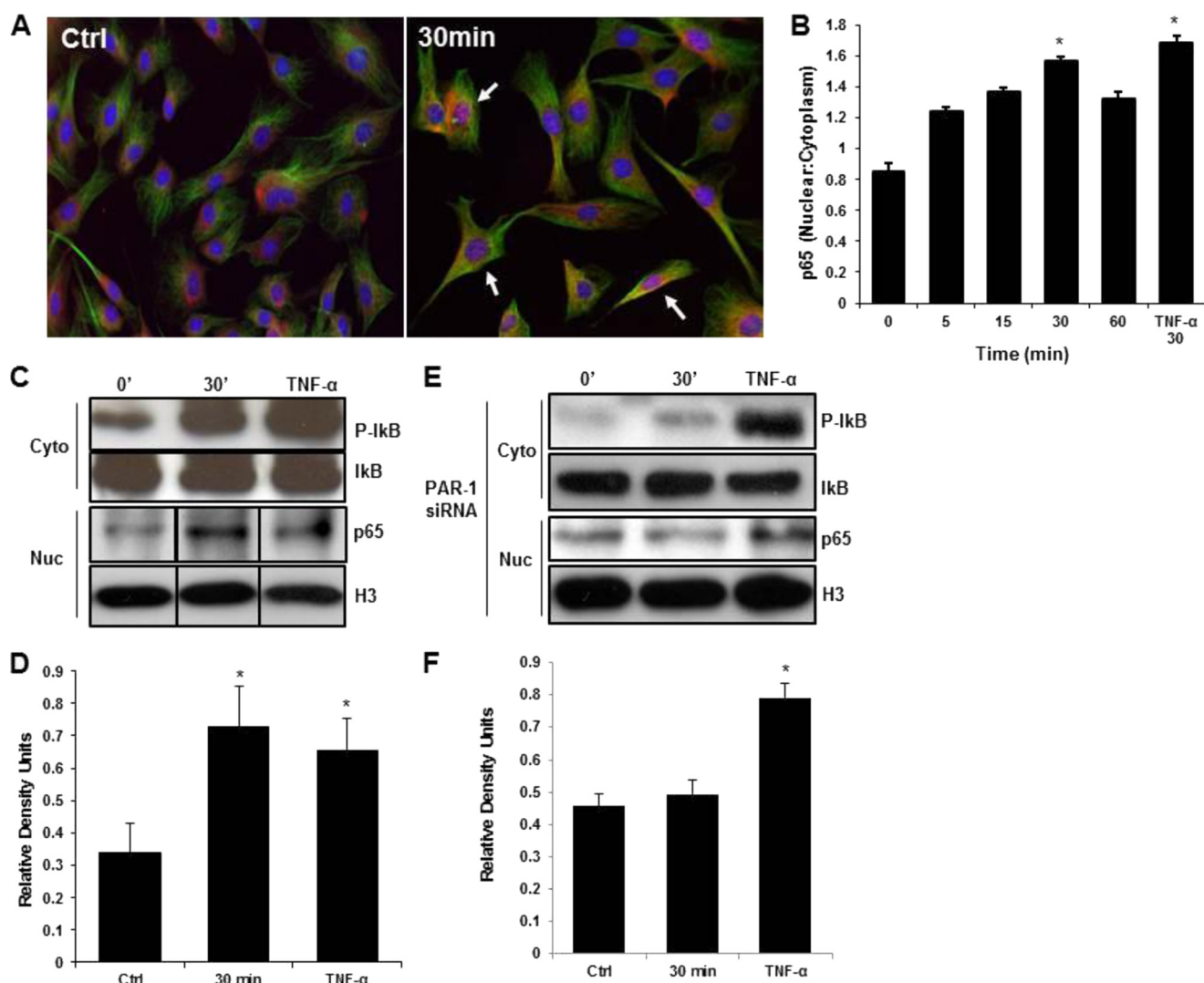
FIGURE 4. **MMP-1 stimulates NF-κB nuclear translocation via a PAR-1-dependent mechanism.** *A,* confocal images representing nuclear and cytoplasmic localization of p65 (*red*) in HUVECs. *Arrows* indicate translocation of p65 transcription factor from the cytoplasm into the nucleus (*red superimposed onto blue*). *Green* represents a β-tubulin counterstain. *B,* quantification of the nuclear to cytoplasmic ratio of p65 staining seen in *A* (*, $p < 0.05$). Western blotting (*C*) and quantification (*D*) of nuclear and cytoplasm fractions from HUVECs following 0 and 30 min of MMP-1 treatment ($n = 3$, *, $p < 0.05$). TNF-α-treated cells serve as a positive control for p65 nuclear translocation. Western blotting (*E*) and quantification (*F*) of nuclear and cytoplasm fractions from HUVECs following 0 and 30 min of MMP-1 treatment in PAR-1 knockdown cells ($n = 3$, *, $p < 0.05$). TNF-α-treated cells serve as a positive control for p65 nuclear translocation.

cell nuclei, a surrogate marker for NF-κB activation (Fig. 4*A*), and the nuclear to cytoplasm ratio of p65 showed a peak at 30 min (0.85 ± 0.05 at $t = 0$ *versus* 1.56 ± 0.03 at $t = 30$ min, $p < 0.05$; Fig. 4*B*). Nuclear separation followed by Western blotting was performed to confirm the nuclear translocation of the p65 subunit following treatment with MMP-1. Phosphorylated IκB levels were markedly higher after MMP-1 treatment (Fig. 4*C*) and the corresponding increase in nuclear p65 is seen as well (Fig. 4, *C* and *D*). TNF-α served as a positive control for p65 nuclear translocation. Similarly to HUVECs, BAECs displayed a similar trend in response to MMP-1 treatment where the ratio of nuclear:cytoplasm p65 was 1.67 ± 0.13 at 30 min compared with 1.24 ± 0.06 in untreated cells (data not shown).

In PAR-1 knockdown cells, levels of p-IκB and nuclear p65 were not different in MMP-1-treated cells compared with controls (Fig. 4, *E* and *F*). TNF-α still causes significant p65 nuclear translocation in PAR-1 knockdown cells (Fig. 4, *E* and *F*).

To test the ability of the p65 subunit of NF-κB to bind and stimulate transcription of the *KDR* gene (*KDR* = VEGFR2-encoding gene), we first searched for NF-κB putative binding sites in the KDR promoter and first intron using TFSEARCH online software. *KDR1* and *KDR2* were located in the first intron and *KDR6* in the upstream region (Fig. 5*A*). Then we used chromatin immunoprecipitation (ChIP) to test the ability of p65 to directly regulate transcription of the *KDR* gene. Upon MMP-1 stimulation there was elevated binding of p65 to the KDR first intron (*KDR1* and *KDR2*) and *KDR* upstream region (*KDR6*) compared with untreated cells (Fig. 5*B*). To discern whether the *KDR* gene was also being actively transcribed, these same genomic regions were analyzed in the chromatin precipitated with anti-acetylated histone H3 antibody. All three promoter regions had higher levels of acetylated histone after MMP-1 stimulation (Fig. 5*C*), indicating elevated levels of *KDR* gene transcription.
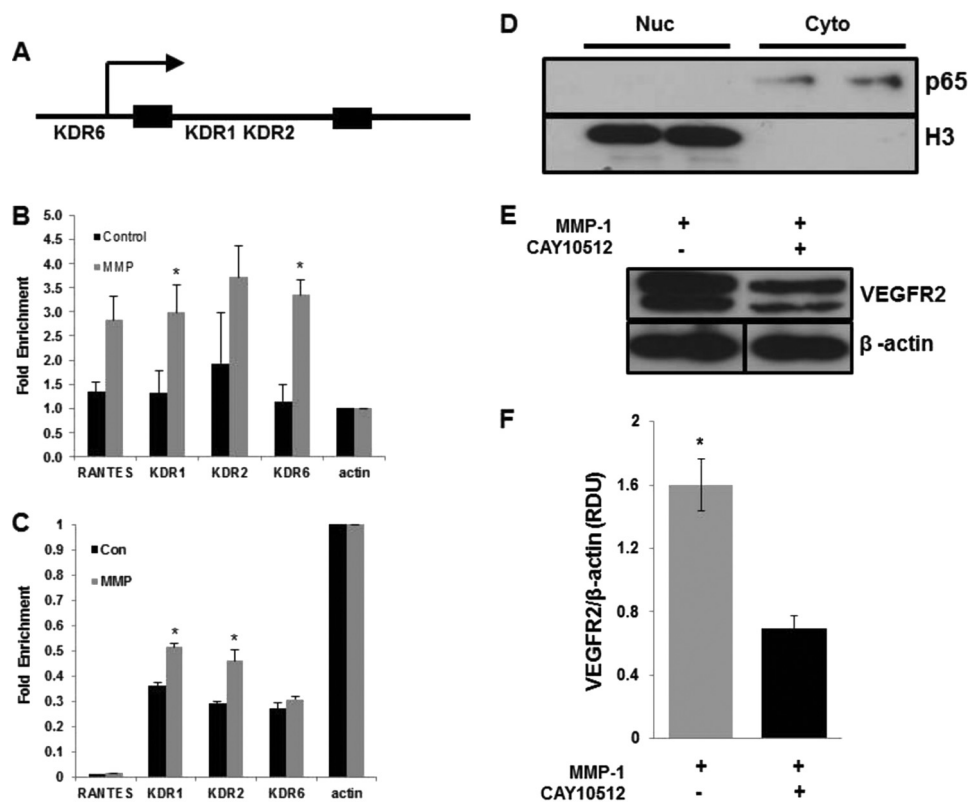
FIGURE 5. **NF-κB-mediates *KDR* gene transcription and VEGFR2 protein levels upon MMP-1 treatment.** *A,* schematic picture of the *KDR* (*KDR* = VEGFR2-encoding gene) with *KDR1* and *KDR2* localized in the first intron and *KDR6* in the upstream region. *B*, chromatin immunoprecipitation of p65 bound to positive control (RANTES), actin, and *KDR* promoters before and after MMP-1 stimulation ($n = 3$, *, $p < 0.05$). *C,* quantification of the precipitated acetylated histone, which serves as a marker for active transcription of the *KDR* gene ($n = 3$; *, $p < 0.05$). *D,* Western blot of nuclear and cytoplasm fractions from HUVECs treated with NF-κB inhibitor as described under "Experimental Procedures." Notice that the inhibitor prevents p65 translocation to the nuclei otherwise observed in MMP-1-treated cells (Fig. 4). *E,* Western blotting and quantification (*F*) of VEGFR2 levels from HUVECs following 24 h of MMP-1 treatment with (*black bar*) and without (*gray bar*) NF-κB inhibitor ($n = 3$, *, $p < 0.05$).

Finally, to test whether the activation of NF-κB observed after MMP-1 treatment is responsible for the increased VEGFR2 levels, we treated the cells with a potent NF-κB inhibitor. Our results (Fig. 5, *D* and *E*) show that in NF-κB inhibited cells, the levels of VEGFR2 were significantly lower compared with control cells following MMP-1 treatment (0.69 ± 0.07 *versus* 1.6 ± 0.16; $n = 3$).

Enhancement of VEGFR2 Levels Are MMP-1-specific and Concentration and Activity Dependent

The ability of MMP-1, -8, and -9 to stimulate VEGFR2 production in endothelial cells was tested. Cells incubated with MMP-1 consistently displayed significantly elevated VEGFR2 levels compared with control cells and cells treated with MMP-8 or -9 (data not shown). Although a wide range of MMP-1 concentrations (applied for 24 h) stimulated VEGFR2 production, 25 ng/ml consistently stimulated the largest increase in VEGFR2 levels compared with untreated controls (Fig. 6*A*). To assess whether MMP-1 itself or its activity is responsible for stimulating the rise in VEGFR2 levels, we incubated endothelial cells with inactive MMP-1 and analyzed VEGFR2 levels in a time-dependent fashion using high throughput imaging (Fig. 6*B*). There was no significant difference in VEGFR2 levels in cells treated with inactivated MMP-1 compared with untreated cells, suggesting that MMP-1 activity is responsible for enhanced VEGFR2 levels.

DISCUSSION

In this study we show that stimulation of endothelial cells with MMP-1 results in elevated VEGFR2 levels. This augmented VEGFR2 expression is then associated with increased VEGF-A-dependent signaling and cell proliferation. We further demonstrate that MMP-1-mediated VEGFR2 production involves activation of PAR-1 and occurs through an NF-κB-dependent mechanism.

VEGFR2 and MMPs are known to have critical roles in a wide variety of normal and pathophysiological conditions, including cell proliferation, vascular remodeling, angiogenesis, tumor progression, chronic inflammation, wound healing, etc. (1–8, 11–13, 29). MMP-1 is an active player in the above conditions; specifically it has been shown to be a prognostic indicator for a variety of cancers (15–20), a biomarker in venous disease (21–23), and to have a role in modulating endothelial permeability by regulation of junctional integrity (4–6). Moreover we have previously demonstrated an early release of active MMPs (including MMP-1) *in vivo* by endothelial cells subjected to increased pressure in combination with decreased shear stress (23). We also showed that MMPs-8 and -9 were released by endothelial cells in this model, and as such we sought to test the effects all three MMPs have on endothelial cells. We found that MMP-8 and -9 had a weak effect on VEGFR2 levels (not as robust as MMP-1) and thus focused our efforts on the demonstrated effects of MMP-1.
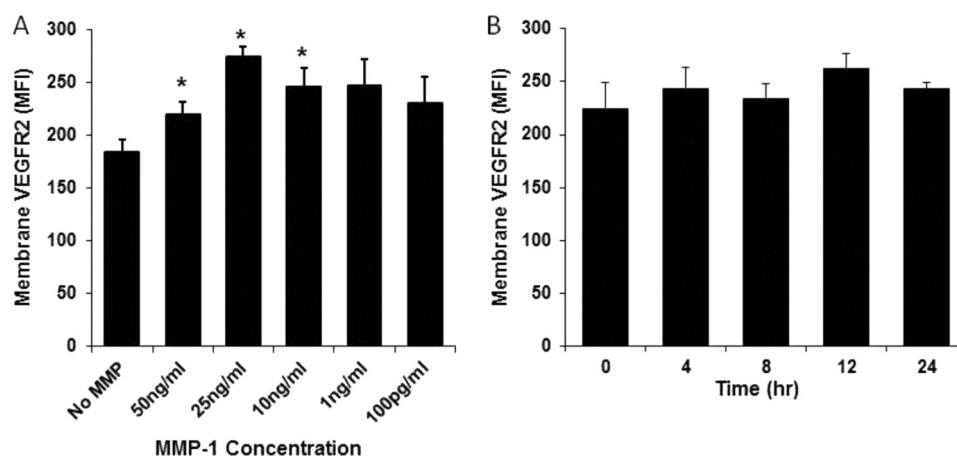
FIGURE 6. **The increase of VEGFR2 levels is dependent on MMP-1 concentration and activity.** High throughput confocal laser scanning analysis of membrane VEGFR2 mean fluorescent intensity (*MFI*) before and after incubation with different concentrations of MMP-1 (*A*) and (*B*) after treatment with inactive MMP-1 (~500 cells/well were counted in the analysis, $n = 4$, *, $p < 0.05$).

VEGFR2 is a principal receptor responsible for modulating endothelial functions such as cell survival, proliferation, and permeability (9–11). Because MMP-1 and VEGFR2 are co-expressed in a variety of settings (9, 10, 21–23), it is intriguing to consider that MMP-1 may have a larger role in priming or sensitizing endothelial cells for functions mediated by VEGFR2. Indeed, pretreatment of endothelial cells with MMP-1 caused a significant elevation of both mRNA and protein levels of VEGFR2. This increased activity was associated with the enhanced VEGF-A-mediated signaling response and accelerated cellular proliferation, confirming that the newly synthesized receptors were functional. This evidence suggests a framework whereby interaction of MMP-1 with endothelial cells may sensitize them to VEGF-A through up-regulation of VEGFR2.

To address a possible mechanism by which MMP-1 may stimulate an increase in VEGFR2 levels we focused on PAR-1, a G-protein coupled receptor involved in the coagulation cascade that is also known to have a role in vascular development (24–28). Griffin *et al.* (24) demonstrated that $Par-1^{-/-}$ mouse embryos frequently died midgestation and displayed abnormal yolk sac vasculature. Transgenic reintroduction of PAR-1 via the endothelial specific promoter prevented death of $Par-1^{-/-}$ embryos, suggesting that PAR-1 is significantly involved with endothelial cell function and blood vessel development. The activation of PAR-1 by the serine protease thrombin has also been shown to enhance endothelial levels of VEGFR2 (28), further suggesting a key role for PAR-1 in endothelial cell functions. Similarly to thrombin, MMP-1 is also able to proteolytically activate PAR-1, subsequently promoting processes such as endothelial cell activation, permeability, and angiogenesis (30–34). However, whereas MMP-1 and thrombin are both able to induce the expression of pro-angiogenic genes in microvascular endothelial cells, MMP-1, but not thrombin, is able to stimulate the production of *VEGF-A* (34). This evidence underscores the importance of MMP-1-mediated up-regulation of VEGFR2 and suggests a positive feedback mechanism by which MMP-1 augments VEGFR2 levels as well as VEGF-A production and release, thereby amplifying endothelial responses. It has to be emphasized that whereas our experimental set up showed that

MMP-1 up-regulates VEGFR2 through a PAR-1 mechanism, it is plausible that other enzymes can also activate PAR-1 and increase VEGFR2 levels.

To determine whether activation of PAR-1 by MMP-1 is required for elevation of VEGFR2 levels we knocked down PAR-1 in endothelial cells and subsequently treated them with MMP-1. We found significantly lower VEGFR2 levels in PAR-1 knockdown cells compared with controls. This result confirms our hypothesis that MMP-1 exerts an effect on PAR-1 to mediate the increase in VEGFR2 levels.

Interestingly, our studies showed that MMP-1 stimulation causes VEGFR2 mRNA elevation at 30 min and 8 h, with protein levels consistently increasing in a time-dependent fashion. This response may be due to the kinetics of PAR-1 cleavage during the 24-h incubation with MMP-1 and due to changes in mRNA:protein turnover. Because it was shown that MMP-1 cleaves PAR-1 at a slower rate than thrombin (35), the time frame in which we see VEGFR2 mRNA and protein elevation is consistent with the kinetics reported for PAR-1 cleavage by MMP-1.

Although PAR-1 knockdown decreased the MMP-1-mediated increase in VEGFR2 levels, the levels of the receptor were still elevated after 24 h of MMP-1 treatment compared with controls. This result may be attributed to an indirect effect of MMP-1. For example, in our model there may be cleavage of extracellular matrix proteins by MMP-1 that work in a paracrine fashion to up-regulate VEGFR2. MMP-1 may also exert an effect on receptors other than PAR-1, thereby also stimulating an elevation in VEGFR2 levels. Because of its role in endothelial proliferation (7), we decided to focus on ERK signaling to determine whether or not the decrease in VEGFR2 seen following PAR-1 knockdown also had an effect on *p*-ERK levels. Indeed, when measuring the effect of PAR-1 knockdown on VEGF-A-mediated signaling we found that *p*-ERK levels were consequently lower, thereby further supporting our conclusion that MMP-1 sensitizes endothelial cell functions by activating PAR-1 and augmenting VEGFR2 levels. The mechanism leading to increased expression of VEGFR2 in response to MMP-1 stimulation was also investigated in this study. It was previously shown that thrombin (a main activator of PAR-1) is able to

stimulate NF-κB and cause the up-regulation of multiple receptors (36, 37). NF-κB has also been shown to mediate *KDR* transcription (38). Furthermore, stimulation of endothelial cells with the inflammatory cytokine TNF-α (a major activator of NF-κB signaling (39)) has been shown to promote the up-regulation of VEGFR2 (40). Collectively these data implicate the involvement of NF-κB in mediating VEGFR2 expression. Therefore, we chose to examine whether NF-κB is directly involved in the endothelial up-regulation of VEGFR2 expression following stimulation with MMP-1. We found that MMP-1 did activate the NF-κB pathway, which then resulted in specific binding of its p65 subunit to the *KDR*/*VEGFR2* promoter, followed by active transcription of *VEGFR2*. The MMP-1-stimulated nuclear translocation of p65 is attenuated by PAR-1 knockdown, and consequently VEGFR2 production is also reduced in these cells. Moreover, the use of a specific NF-κB inhibitor blunted the elevation in VEGFR2 levels. Altogether, these results demonstrate not only the ability of NF-κB to bind the *KDR* promoter, but also that NF-κB is a major mediator of MMP-1-induced VEGFR2 up-regulation and expression.

Interactions between MMP-1 and endothelial cells are found in many physiological and pathophysiological conditions. In some cancers MMP-1 is highly expressed (often times in levels equal to or greater than the concentration we used in these studies (41)) and can influence vascularization of tissue in the tumor microenvironment, thus facilitating angiogenesis and disease progression (42). Among others, a PAR-1/MMP-1 signaling axis has been shown to facilitate the formation of metastatically competent melanoma (34). In other pathologies, VEGFR2, PAR-1, and MMPs collectively have been shown to contribute to endothelial barrier regulation, facilitating transmigration of leukocytes into the surrounding milieu (4–6). Therefore our results suggest that MMP-1-mediated up-regulation of VEGFR2 may be an important modulator of a variety of endothelial functions presented above. Overall, the results presented in this study propose a mechanism by which the interaction between MMP-1 and PAR-1 on endothelial cells promotes expression of VEGFR2, thereby sensitizing endothelial cells for a variety of functions mediated by this receptor.

REFERENCES

1. Egeblad, M., and Werb, Z. (2002) New functions for the matrix metalloproteinases in cancer progression. *Nat. Rev. Cancer* **2,** 161–174
2. Stamenkovic, I. (2003) Extracellular matrix remodeling. The role of matrix metalloproteinases. *J. Pathol.* **200,** 448–464
3. Kessenbrock, K., Plaks, V., and Werb, Z. (2010) Matrix metalloproteinases. Regulators of the tumor microenvironment. *Cell* **141,** 52–67
4. Alexander, J. S., and Elrod, J. W. (2002) Extracellular matrix, junctional integrity and matrix metalloproteinase interactions in endothelial permeability regulation. *J. Anat.* **200,** 561–574
5. Carden, D., Xiao, F., Moak, C., Willis, B. H., Robinson-Jackson, S., and Alexander, S. (1998) Neutrophil elastase promotes lung microvascular injury and proteolysis of endothelial cadeherins. *Am. J. Physiol.* **275,** H385-H392
6. Wachtel, M., Frei, K., Ehler, E., Fontana, A., Winterhalter, K., and Gloor S. M. (1999) Occludin proteolysis and increased permeability in endothelial cells through tyrosine phosphatase inhibition. *J. Cell Sci.* **112,** 4347–4356
7. Secchiero, P., Gonelli, A., Carnevale, E., Milani, D., Pandolfi, A., Zella, D., and Zauli, G. (2003) TRAIL promotes the survival and proliferation of primary human vascular endothelial cells by activating the Akt and ERK pathways. *Circulation* **107,** 2250–2256
8. Rundhaug, J. E. (2005) Matrix metalloproteinases and angiogenesis. *J. Cell Mol. Med.* **9,** 267–285
9. Carmeliet, P., and Jain, R. K. (2000) Angiogenesis in cancer and other diseases. *Nature* **407,** 249–257
10. Veikkola, T., Karkkainen, M., and Claesson-Welsh, L. (2000) Regulation of angiogenesis via vascular endothelial growth factor receptors. *Cancer Res.* **60,** 203–212
11. Olsson, A. K., Dimberg, A., Kreuger, J., and Claesson-Welsh, L. (2006) VEGF receptor signaling. In control of vascular function. *Nat. Rev. Mol. Cell Biol.* **7,** 359–371
12. Breslin, J. W., Pappas, P. J., Cerveira, J. J., Hobson, R. W., 2nd, and Duran, W. N. (2003) VEGF increases endothelial permeability by separate signaling pathways involving ERK-1/2 and nitric oxide. *Am. J. Physiol. Heart Circ.* **284,** H92–100
13. Uchida, C., Gee, E., Ispanovic, E., and Haas, T. L. (2008) JNK as a positive regulator of angiogenic potential in endothelial cells. *Cell Biol. Int.* **32,** 769–776
14. Mavria, G., Vercoulen, Y., Yeo, M., Paterson, H., Karasarides, M., Marais, R., Bird, D., and Marshall, C. J. (2006) ERK-MAPK signaling opposes Rho-kinase to promote endothelial cell survival and sprouting during angiogenesis. *Cancer Cell* **9,** 33–44
15. Murray, G. I., Duncan, M. E., O'Neil, P., Melvin, W. T., and Fothergill, J. E. (1996) Matrix metalloproteinase-1 is associated with poor prognosis in colorectal cancer. *Nat. Med.* **2,** 461–462
16. Inoue, T., Yashiro, M., Nishimura, S., Maeda, K., Sawada, T., Ogawa, Y., Sowa, M., and Chung, K. H. (1999) Matrix metalloproteinase-1 expression is a prognostic factor for patients with advanced gastric cancer. *Int. J. Mol. Med.* **4,** 73–77
17. Murray, G. I., Duncan, M. E., O'Neil, P., McKay, J. A., Melvin, W. T., and Fothergill, J. E. (1998) Matrix metalloproteinase-1 is associated with poor prognosis in oesophageal cancer. *J. Pathol.* **185,** 256–261
18. Ito, T., Ito, M., Shiozawa, J., Naito, S., Kanematsu, T., and Sekine, I. (1999) Expression of the MMP-1 in human pancreatic carcinoma. Relationship with prognostic factor. *Mod. Pathol.* **12,** 669–674
19. Nakopoulou, L., Giannopoulou, I., Gakiopoulou, H., Liapis, H., Tzonou, A., and Davaris, P. S. (1999) Matrix metalloproteinase-1 and -3 in breast cancer. Correlation with progesterone receptors and other clinicopathological feature. *Hum. Pathol.* **30,** 436–442
20. Poola, I., DeWitty, R. L., Marshalleck, J. J., Bhatnagar, R., Abraham, J., and Leffall, L. D. (2005) Identification of MMP-1 as a putative breast cancer predictive marker by global gene expression analysis. *Nat. Med.* **11,** 481–483
21. Buján, J., Jurado, F., and Gimeno, M. J. (2000) Changes in metalloproteinase (mmp-1, mmp-2) expression in the proximal region of the varicose saphenous vein in young subjects. *Phlebology* **15,** 64–70
22. Woodside, K. J., Hu, M., Burke, A., Murakami, M., Pounds, L. L., Killewich, L. A., Daller, J. A., and Hunter, G. C. (2003) Morphologic characteristics of varicose veins. Possible role of metalloproteinases. *J. Vasc. Surg.* **38,** 162–169
23. Alsaigh, T., Pocock, E. S., Bergan, J. J., and Schmid-Schönbein, G. W. (2011) Acute venous occlusion enhances matrix metalloprotease activity. Implications on endothelial dysfunction. *Microvasc. Res.* **81,** 108–116
24. Griffin, C. T., Srinivasan, Y., Zheng, Y. W., Huang, W., and Coughlin, S. R. (2001) A role for thrombin receptor signaling in endothelial cells during embryonic development. *Science* **293,** 1666–1670
25. Boire, A., Covic, L., Agarwal, A., Jacques, S., Sherifi, S., and Kuliopulos, A. (2005) PAR1 is a matrix metalloproteases-1 receptor that promotes invasion and tumorigenesis of breast cancer cells. *Cell* **120,** 303–313
26. Blackburn, J. S., and Brinckerhoff, C. E. (2008) Matrix metalloproteinase-1 and thrombin differentially activate gene expression in endothelial cells via PAR-1 and promote angiogenesis. *Am. J. Pathol.* **173,** 1736–1746
27. Kim, S. J., Shin, J. Y., Lee, K. D., Bae, Y. K., Choi, I. J., Park, S. H., and Chun,

K. H. (2011) Galectin-3 facilitates cell motility in gastric cancer by up-regulating protease-activated receptor-1 (PAR-1) and matrix metalloproteinase-1 (MMP-1). *PLoS ONE* **6,** e25103

28. Tsopanoglou, N. E., and Maragoudakis, M. E. (1999) On the mechanism of thrombin-induced angiogenesis. *J. Biol. Chem.* **274,** 23969–23976

29. Hanahan, D., and Weinberg, R. A. (2011) Hallmarks of cancer. The next generation. *Cell* **144,** 646–674

30. Klarenbach, S. W., Chipiuk, A., Nelson, R. C., Hollenberg, M. D., and Murray, A. G. (2003) Differential actions of PAR2 and PAR1 in stimulating human endothelial cell exocytosis and permeability. The role of Rho-GTPases. *Circ. Res.* **92,** 272–278

31. Kaneider, N. C., Leger, A. J., Agarwal, A., Nguyen, N., Perides, G., Derian, C., Covic, L., and Kuliopulos, A. (2007) Role reversal for the receptor PAR1 in sepsis-induced vascular damage. *Nat. Immunol.* **8,** 1303–1312

32. Agarwal, A., Covic, L., Sevigny, L. M., Kaneider, N. C., Lazarides, K., Azabdaftari, G., Sharifi, S., and Kuliopulos, A. (2008) Targeting a metalloprotease-PAR1 signaling system with cell-penetrating pepducins inhibits angiogenesis, ascites, and progression of ovarian cancer. *Mol. Cancer Ther.* **7,** 2746–2757

33. Goerge, T., Barg, A., Schnaeker, E. M., Poppelmann, B., Shpacovitch, V., Rattenholl, A., Maaser, C., Luger, T. A., Steinhoff, M., and Schneider, S. W. (2006) Tumor-derived matrix metalloproteinase-1 targets endothelial protease-activated receptor 1 promoting endothelial cell activation. *Cancer Res.* **66,** 7776–7774

34. Blackburn, J. S., Liu, I., Coon, C. I., and Brinckerhoff, C. E. (2009) A matrix metalloproteinase-1/protease activated receptor-1 signaling axis promotes melanoma invasion and metastasis. *Oncogene* **28,** 4237–4248

35. Nesi, A., and Fragai, M. (2007) Substrate specificities of matrix metalloproteinase 1 in PAR-1 exodomain proteolysis. *Chembiochem.* **8,** 1367–1369

36. Tantivejkul, K., Loberg, R. D., Mawocha, S. C., Day, L. L., John, L. S., Pienta, B. A., Rubin, M. A., and Pienta, K. J. (2005) PAR1-mediated NFκB activation promotes survival of prostate cancer cells through a Bcl-xL-dependent mechanism. *J. Cell Biochem.* **96,** 641–652

37. Hsieh, H. L., Tung, W. H., Wu, C. Y., Wang, H. H., Lin, C. C., Wang, T. S., and Yang, C. M. (2009) Thrombin induces EGF receptor expression and cell proliferation via a PKC/c-Src-dependent pathway in vascular smooth muscle cells. *Arterioscler. Thromb. Vasc. Biol.* **29,** 1594–1601

38. Illi, B., Puri, P., Morgante, L., Capogrossi, M. C., and Gaetano, C. (2000) Nuclear factor-κB and cAMP response element-binding protein mediate opposite transcriptional effects on the Flk-1/KDR gene promoter. *Circ. Res.* **86,** E110–117

39. Barnes, P. J., and Karin, M. (1997) Nuclear factor-κB. A pivotal transcription factor in chronic inflammatory diseases. *N. Engl. J. Med.* **336,** 1066–1071

40. Giraudo, E., Primo, L., Audero, E., Gerber, H. P., Koolwijk, P., Soker, S., Klagsbrun, M., Ferrara, N., and Bussolino, F. (1998) Tumor necrosis factor-α regulates expression of vascular endothelial growth factor receptor-2 and of its co-receptor neuropilin-1 in human vascular endothelial cells. *J. Biol. Chem.* **273,** 22128–22135

41. Nikkola, J., Vihinen, P., Vuoristo, M. S., Kellokumpu-Lehtinen, P., Kähäri, V. M., and Pyrhönen, S. (2005) High serum levels of matrix metalloproteinase-9 and matrix metalloproteinase-1 are associated with rapid progression in patients with metastatic melanoma. *Clin. Cancer Res.* **11,** 5158–5166

42. Blackburn, J. S., Rhodes, C. H., Coon, C. I., and Brinckerhoff, C. E. (2007) RNA interference inhibition of matrix metalloproteinase-1 prevents melanoma metastasis by reducing tumor collagenase activity and angiogenesis. *Cancer Res.* **67,** 10849–10858

43. Lee, T. I., Johnstone, S. E., and Young, R. A. (2006) Chromatin immunoprecipitation and microarray-based analysis of protein location. *Nat. Protoc.* **1,** 729–748